Applied Surface Science 341 (2015) 190–195

Contents lists available at ScienceDirect

Applied Surface Science

journal homepage: www.elsevier.com/locate/apsusc

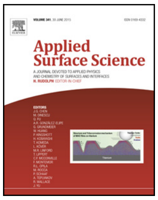

In situ anion-exchange synthesis and photocatalytic activity of AgBr/Ag_2O heterostructure

Yuhui Cao, Qiuye Li*, Yangyang Xing, Lanlan Zong, Jianjun Yang*

Key Laboratory for Special Functional Materials, Henan University, Kaifeng 475004, China

ARTICLE INFO

Article history:
Received 7 January 2015
Received in revised form 23 February 2015
Accepted 25 February 2015
Available online 14 March 2015

Keywords:
AgBr
Ag_2O
Heterostructure
Photocatalytic
Methyl orange
Visible light

ABSTRACT

AgBr/Ag_2O heterostructure photocatalysts were synthesized by a simple in situ anion-exchange route. The ratio of AgBr and Ag_2O in the composites could be easily controlled by adjusting the concentration of NaBr solution. The AgBr/Ag_2O-5 heterostructure exhibited a much higher photocatalytic activity than the pure AgBr and Ag_2O particles in photodegradation of methyl orange (MO) under visible light irradiation. On the basis of the characterization by X-ray diffraction, photoluminescence (XRD), X-ray photoelectron spectroscope (XPS), and UV–vis diffuse reflectance spectra (DRS), a mechanism was proposed to account for the enhanced photocatalytic activity of AgBr/Ag_2O heterostructure.

1. Introduction

Semiconductor photocatalysts have attracted considerable attention due to their great potential in solving current environment and energy problems with abundant solar light [1–4]. During the past decades, various semiconductor materials, including elements (Si, Ge) [5,6], III–V (GaAs, GaP, InP, InAs) compounds [7–9], II–VI (ZnS, ZnSe, CdS, CdSe) compounds [10–12] and oxides (TiO_2, ZnO) [13–15] have been successfully fabricated by diverse techniques, and their novel and unique photocatalytic properties have been extensively explored [16,17]. Although these materials have greatly expanded our ability to construct a wide range of photocatalytic systems, it is worth pointing out that their unsatisfactory activities and low efficiencies in the utilization of the visible light is still highly desirable to be solved for practical applications. Thereby, the exploration and creation of new semiconductor materials as highly efficient photocatalysts is still a great challenge.

More recently, Ag_2O [18,19], Ag_3PO_4 [20,21] and silver halides (AgX, X = Cl, Br, I) are well-known as photosensitive materials and have been extensively used in photographic films and photodegradation of organic pollutants [22–26]. By absorbing the incident light, AgX generate electrons in the conduction band (CB) and holes in the valence band (VB). The photogenerated electrons in the CB are captured by surface lattice Ag^+ ions to form Ag^0 clusters, whereas photogenerated holes in the VB oxidize lattice X^- to release X_2, resulting in the photodecomposition of silver halides and the formation of metallic Ag. Therefore, it is expected that if the photogenerated holes in AgX can transfer to other electron donors (such as organic substances) before oxidizing the lattice X^-, and the photogenerated electrons can be captured by other electron accepters before reducing the lattice Ag^+, it is possible to keep the photo-induced stability of the AgX phase. In our previous studies, we have also reported the highly efficient Ag-based photocatalytic materials such as AgBr/TiO_2, AgBr-TN film, Ag-loaded $BaTiO_3$/TiO_2 [27–29].

Herein, we designed a new system of AgBr/Ag_2O by growth of AgBr nanoshells on the surfaces of Ag_2O particles at room temperature. The insoluble AgBr nanoshells could efficiently protect inner Ag_2O from dissolution in aqueous solutions and improve their stabilities during the photocatalytic process. Moreover, the conduction band and valence band potentials of AgBr are more positive than those of Ag_2O, which could promote the transfer and separation of photoexcited electron–hole pairs through their heterojunctions. Furthermore, the experimental results confirmed that these novel AgBr/Ag_2O heterostructures exhibited much higher photocatalytic activities and stabilities than the pure AgBr and Ag_2O particles.

---

* Corresponding author. Tel.: +86 37123881358.
E-mail addresses: qiuyeli@henu.edu.cn (Q. Li), yangjianjun@henu.edu.cn (J. Yang).

http://dx.doi.org/10.1016/j.apsusc.2015.02.174

2. Experimental

2.1. Preparation of Ag_2O nanoparticles and $AgBr/Ag_2O$ heterostructures

Ag_2O nanoparticles were prepared by a simple co-precipitation reaction between Ag^+ and OH^- ions in distilled water. In a typical synthesis, 50 mL of $AgNO_3$ aqueous solution was poured into 50 mL of NaOH aqueous solution with stirring. After the solution was incubated at room temperature for 1 h in dark, the dark precipitate was collected, rinsed with distilled water, and dried at room temperature to obtain Ag_2O nanoparticles.

$AgBr/Ag_2O$ heterostructures were prepared by the obtained Ag_2O nanoparticles were further reacted with appropriate sodium bromide (0.2 M). In such a process, Ag_2O particles were used as both template and silver ion source. The surface of Ag_2O particles could be readily reacted with bromide ions to form AgBr nanoparticles, and thereby $AgBr/Ag_2O$ heterostructures were synthesized. According to this method, different mass ratio of $AgBr/Ag_2O$ samples were obtained, and the samples were denoted as $AgBr/Ag_2O$-x (x means the mass percentage of AgBr). The reference AgBr was obtained by the simple co-precipitation reaction of $AgNO_3$ and NaBr solution.

2.2. Characterizations

X-ray diffraction (XRD) patterns were obtained on a Philips X'Pert Pro X-ray diffractometer (Holland) (Cu Kα radiation, 2θ range 10–90°, scan step size 0.08°, time per step 1.0 s, generator voltage 40 kV, tube current 40 mA). The morphologies of the samples were taken by SEM (JSM-7100F, JEOL Co., Japan) and TEM (JEM-2100, JEOL Co., Japan). Diffused reflectance spectra (DRS) were obtained by a UV–VIS spectrophotometer (UV-3010, Shimadzu, Japan), using $BaSO_4$ as a reference. Surface composition and chemical states were analyzed with a Thermo escalab 250Xi X-ray photoelectron spectroscope (XPS) equipped with Al Kα radiation, and the binding energy was calibrated by the C 1s peak (284.6 eV) of the contamination carbon. The Brunauer–Emmett–Teller (BET) surface areas were measured by automatic surface area (QUADRASORB SI). The photoluminescence (PL) spectra were recorded on a F-7000 FL Spectrophotometer.

2.3. Evaluation of the photocatalytic activity

Methyl orange (MO) was selected as the model chemicals to evaluate the photocatalytic activity of the samples. In a typical experiment, the samples (0.1 g) were put into a quartz reactor containing 100 mL MO aqueous solution (20 mg/L). Prior to irradiation, the suspension was magnetically stirred in dark for 1 h to establish an adsorption–desorption equilibrium. A 300 W Xe arc lamp with a 420 cutoff filter was used as the visible light source ($\lambda \geq 420$ nm). The degradation of MO dye was detected using a UV–vis spectrophotometer (722, Shanghai Jingke Instrument Plant, China).

3. Results and discussion

3.1. Structural and morphological study of the catalysts

The SEM image of Ag_2O of Fig. 1a showed that the particles sizes of Ag_2O were not uniform, and the large particles were consisted by many little ones. From Fig. 1b and c, we can clearly see that the particles sizes of $AgBr/Ag_2O$ heterostructures were only 20–50 nm. The $AgBr/Ag_2O$ heterostructure particles decreased apparently than the pure Ag_2O particles, indicating that some large Ag_2O particles has transformed to the small AgBr particles. The HRTEM images of the composites showed two different lattice fringes, one of the interplanar spacing of 0.27 nm was corresponded to (1 1 1) plane of Ag_2O (JCPDS 41-1104) [30], and the another of 0.145 nm was indexed to (400) plane of AgBr (JCPDS 06-4308). The EDS spectrum illustrated the existence of AgBr, and the mass ratio of AgBr and Ag_2O was 3.3%, which is smaller than the designed value. In addition, surface areas of the $AgBr/Ag_2O$-5 and Ag_2O samples are 19.5 $m^2\,g^{-1}$ and 16.8 $m^2\,g^{-1}$, which were investigated by N_2 adsorption–desorption isotherm. The two values were not large difference, indicating that the BET surface areas should not be the major factor in affecting the photocatalytic activity.

Fig. 2 showed XRD patterns of the as-prepared $AgBr/Ag_2O$ heterostructures with different AgBr contents. The diffraction peaks of pure Ag_2O at 32.8°, 38.1°, 55.0°, 65.4°, 68.7° are indexed to the (1 1 1), (2 0 0), (2 2 0), (3 1 1) and (2 2 2) planes of the cubic crystal phase (JCPDS 72-2108). Patterns a and b illustrated that the characteristic peaks of Ag_2O (1 1 1) and AgBr (2 0 0) were around at 32.8° and 30.9°, respectively [31,32]. When $AgBr/Ag_2O$ heterostructures were formed by the ion-exchange method, the XRD patterns changed correspondingly. As shown in pattern c, some weak peaks ascribed to AgBr emerged with Ag_2O phase, which should be due to the low content of AgBr. With increasing AgBr content, the intensity of the diffraction peaks at 26.8°, 30.9°, 44.3°, 55.0° and 64.5° increased gradually, and the peaks were assigned to the (1 1 1), (2 0 0), (2 2 0), (2 2 2) and (4 0 0) crystal planes of AgBr (JCPDS 06-4308). These observations indicated the successful grafting of AgBr onto Ag_2O nanoparticles.

3.2. Elemental chemical status of the catalysts

In order to further confirm the composition and chemical species/states of $AgBr/Ag_2O$ heterostructures, the X-ray photoelectron spectroscopy (XPS) of the samples was conducted. As seen in Fig. 3a, the binding energy of Ag 3d3/2 and Ag 3d5/2 centered at 368.5 and 374.5 eV are highly consistent with the values reported for Ag^+ [33]. And no apparent peaks belonging to the Ag^0 appeared, indicating that the $AgBr/Ag_2O$ heterostructures was rather stable. Fig. 3b shows the XPS spectrum of the O 1s region of $AgBr/Ag_2O$-5, which can be fitted by two peaks. The O 1s peak consisted of a dominant peak at 531.5 eV and another higher energy peaks at approximately 530.7 eV. The two peaks can be indexed to Ag—O bonding and O—H in the hydroxyl groups (such as absorbed H_2O) [33,34] on the surface of doped $AgBr/Ag_2O$-5, respectively. The peak at 69.4 eV was ascribed to Br 3d [35] in inset of Fig. 3b. The result also clearly indicates the presence of AgBr, implying the formation of $AgBr/Ag_2O$ heterojunctions.

3.3. Optical properties of the photocatalysts

The UV–vis DRS spectra of $AgBr/Ag_2O$ heterostructures are illustrated in Fig. 4. The absorption onset of the pure AgBr was 476 nm, which corresponded to 2.61 eV of the band gap. While the pure brownish black Ag_2O nanoparticles showed strong absorption both in ultraviolet and visible-light region that should be due to its narrower band gap (1.2 eV) [36]. After loading in the range of 5–20 at% of AgBr nanoparticles on the Ag_2O, there are slight increase in the visible-light absorption due to a limited amount of AgBr nanoparticles, while the absorption in the ultraviolet region increased apparently. When the amount of AgBr nanoparticles is 100 at%, its UV–vis spectra showed a similar but stronger absorption at 400–500 nm compared with pure AgBr, which may be owing to the smaller AgBr nanoparticles obtained by the ion-exchanged method.